

Emodin-Loaded PLGA-TPGS Nanoparticles Combined with Heparin Sodium-Loaded PLGA-TPGS Nanoparticles to Enhance Chemotherapeutic Efficacy Against Liver Cancer

Hongyan Liu¹ · Hong Xu² · Chenghong Zhang² · Meng Gao¹ · Xiaoguang Gao¹ · Chuchu Ma¹ · Li Lv¹ · Dongyan Gao¹ · Sa Deng¹ · Changyuan Wang¹ · Yan Tian¹

Received: 4 May 2016 / Accepted: 29 July 2016 / Published online: 10 August 2016
© Springer Science+Business Media New York 2016

ABSTRACT

Purpose Heparin sodium (HS)-loaded poly(lactic-co-glycolic acid)-D- α -tocopheryl polyethylene glycol 1000 succinate (PLGA-TPGS) nanoparticles (HPTNs) were prepared as a sustained and targeting delivery carrier and combined with emodin (EMO)-loaded PLGA-TPGS nanoparticles (EPTNs), which were investigated previously to form a combination therapy system for the treatment of liver cancer.

Methods To assess cellular uptake and evaluate the liver-targeting capacity by analyzing the drug concentrations and frozen slices, HS/eosin-loaded PLGA-TPGS nanoparticles, HS/fluorescein-loaded PLGA-TPGS nanoparticles and EMO/C6-loaded PLGA-TPGS nanoparticles, which contained eosin, fluorescein and C6 as fluorescent probes, respectively, were also prepared. All of these nanoparticles were characterized in terms of their size, size distribution, surface charge, drug loading, encapsulation efficiency, *in vitro* release profile and cellular uptake. The apoptosis of HepG2 cells induced by EPTNs in combination with HPTNs was determined by Annexin V-FITC staining and PI labelling.

Results Transmission electron microscopy indicated that these nanoparticles were stably dispersed spheres with sizes ranging from 100 to 200 nm. The results demonstrated that fluorescent nanoparticles were internalized into HepG2 and HCa-F cells efficiently and had improved liver-targeting properties. The combination of EPTNs and HPTNs effectively

inhibited cell growth *in vitro* and had a remarkable synergistic anticancer effect *in vivo*. EPTNs combined with HPTNs induced HepG2 cell apoptosis with synergistic effects. The liver H&E slice images of a hepatocarcinogenic mouse model indicated that EPTNs in combination with HPTNs significantly suppressed tumour growth *in vivo*.

Conclusions The research suggests that the combination therapy system of EPTNs and HPTNs could be a new direction for liver cancer therapy.

KEY WORDS combination therapy · emodin · heparin sodium · liver cancer · PLGA-TPGS nanoparticles

ABBREVIATIONS

AUC	Area under concentration-time curve
BPTN	Blank PLGA-TPGS nanoparticles
C6	Coumarin-6
DAPI	4, 6-diamidino- 2-phenylindole dihydrochloride
DEN	Diethylnitrosamine
DL	Drug loading
ECPTN	EMO/coumarin-6-loaded PLGA-TPGS nanoparticles
EE	Encapsulation efficiency
EM&HSS	EMO combined with HS solutions
EMO	Emodin
EMS	Emodin solutions
EPTN	EMO-loaded PLGA-TPGS nanoparticles
FS	5-Fluorouracil solutions
H&E staining	Hematoxylin-eosin staining
HCC	Hepatocellular carcinoma
HEPTN	HS/Eosin-loaded PLGA-TPGS nanoparticles
HFPTN	HS/Fluorescein-loaded PLGA-TPGS nanoparticles

Electronic supplementary material The online version of this article (doi:10.1007/s11095-016-2010-5) contains supplementary material, which is available to authorized users.

✉ Yan Tian
tiany2004@126.com

¹ College of Pharmacy, Dalian Medical University, Dalian 116044, China

² College of Basic Medical Sciences, Dalian Medical University, Dalian 116044, China

HPTN	HS-loaded PLGA-TPGS nanoparticles
HS	Heparin sodium
HSS	Heparin sodium solutions
IR	inhibition ratio
MDR	Multiple drug resistance
NPs	Nanoparticles
PDI	Polydispersity index
PI	3,8-Diamino-5-[3-(diethylmethylammonium) propyl]-6-phenylphenanthridinium diiodide
PLGA	Poly(lactic-co-glycolic acid)
PLGA-TPGS	Poly(lactic-co-glycolic acid)-d- α -tocopheryl polyethylene glycol 1000 succinate
Re	Relative targeting efficiency
SDS	Sodium dodecyl sulphate
SI	Selectivity index
TCMs	Traditional Chinese medicines
Te	Targeting efficiency
TI	Targeting index
TPGS	D- α -tocopheryl polyethylene glycol 1000 succinate
WST-1	4-[3-(4-iodophenyl)-2-(4-nitrophenyl)-2H-5-tetrazolio]-1,3-benzene sulphonate)

INTRODUCTION

Hepatocellular carcinoma (HCC) is one of the most common malignant tumours in China; approximately 11 million people die each year from HCC, which reflects an increasing trend in recent years (1,2). Although clinical research on HCC has made great progress, the annual number of deaths due to HCC is higher than that of other malignant tumours because of its high recurrence and high transfer rate (3,4). Therefore, molecular targeted therapy, such as anti-epidermal growth factor receptor drugs and multi-target inhibitors, has become a new research focus in the treatment of HCC (5,6). In addition, many traditional Chinese medicines (TCMs) have been used clinically for cancer treatment. The primary focus in the present stage of our research is how to increase the curative effects of TCMs for the treatment of liver cancer, which could aid in the development of these TCMs into molecular targeted drugs to reduce the disadvantages of the conventional chemotherapeutic scheme. The metastasis and recurrence of HCC is a very complex process that includes cancer invasion, metastasis, and angiogenesis. Most studies have focused on the cancer cells, but the tumour microenvironment is increasingly appreciated due to the rapid development of tumour molecular biology. Therefore, combining different drugs for the treatment of liver cancer has become a more popular research direction (7). For example,

it was reported that HS-conjugated pluronic nanogels used as multi-drug nanocarriers had the potential to deliver multi-therapeutic agents with different characteristics for cancer chemotherapy (8). Another study illustrated that triptorelin (Decapeptyl) combined with heparin could significantly decrease the conversion of estrone sulfate (E_1S) to estradiol (E_2) in MCF-7 cells, which suggested a new possibility for the control of E_2 in hormone-dependent breast cancer (9).

Heparin sodium (HS), which is found in the liver, is extracted primarily from the intestinal mucosa of cows or pigs. HS is well known as an anticoagulant, but it also has many other biological activities; in particular, an anticancer effect has attracted the interest of researchers (10). The present study showed that HS could be combined with a variety of proteins in the tumour microenvironment to exert an anticancer effect. This effect was thought to be related to the inhibition of a variety of proteins in the tumour microenvironment that altered the phenotype of the cancer cells. In contrast, HS could inhibit angiogenesis in cancer by combining with the epidermal growth factor receptor (EGFR) (11). At the same time, HS can also inhibit heparinase activity. Heparinase is a glucuronidase that breaks the heparin sulfate chains on the cell surface and in the extracellular matrix, and it can accelerate the growth and metastasis of cancer by releasing angiogenic factors, such as vascular endothelial growth factor (VEGF), basic fibroblast growth factor (bFGF), etc. Consequently, the discovery of heparinase has become another potential target in the treatment of cancer (12). The present research has shown clearly that the clinical application of different drugs combined with HS could significantly prolong the survival of cancer patients (13). However, HS has strong anticoagulant activity. If HS were used over the long term, it would cause problems, such as tolerance, pain, injury, skin hematoma, and decreased platelets. Consequently, HS in combination with chemotherapeutic drugs has only been used as an anti-thrombotic for patients undergoing clinical cancer treatment; it has not yet been used formally as an anticancer drug.

In view of the present research situation and the development trends in the treatment of liver cancer, our study will combine emodin (EMO) with HS to enhance liver cancer therapy. EMO primarily targets the growth of the cancer cells, whereas HS acts on the tumour microenvironment and inhibits the angiogenesis of HCC.

EMO is extracted from rhubarb, and it has a specific inhibitory effect on the development and progression of a variety of cancer cells, such as breast cancer cells and liver cancer cells (14). In our previous work, EMO-loaded nanoparticles (NPs) were prepared to improve therapeutic efficacy by ameliorating the poor water solubility and lipid solubility of EMO (15). Poly lactic-co-glycolic acid (PLGA) is a biodegradable polymer that is approved by the Food and Drug Administration (FDA); it has good biocompatibility, non-toxic, non-stimulatory, and non-immunogenic (16). D- α -

tocopheryl polyethylene glycol 1000 succinate (TPGS) is a water-soluble derivative of vitamin E that is widely used as an emulsifier, solvent, and additive in drug delivery (17). TPGS could improve the permeability of the cell membrane to enhance the absorption of drugs and effectively inhibit the growth of cancer cells (18). PLGA and TPGS have been used in multiple pharmaceutical products and drug delivery systems. Poly (lactic-co-glycolic acid)-d- α -tocopheryl polyethylene glycol 1000 succinate (PLGA-TPGS) was synthesized from PLGA and TPGS; the synthetic process and $^1\text{H-NMR}$ spectrum can be found in our previous study using a formerly described method to prepare NPs as carrier materials (19,20). With PLGA-TPGS as the NP carrier, EMO combined with HS can better target liver cancer. This improved targeting occurs because TPGS is an excellent solubilizer, emulsifier, bioavailability enhancer for hydrophobic drugs, and reduce the P-glycoprotein (P-gp)-mediated multiple drug resistance (MDR) of tumour cells, which can also enhance the *in vivo* uptake of NPs; as a result, the NPs were more easily ingested by liver cancer cells (21,22). Furthermore, the drugs can be released from the carrier more quickly and completely because PLGA-TPGS has lower molecular weight and higher hydrophilicity.

In this research, EMO-loaded PLGA-TPGS NPs (EPTNs) and HS-loaded PLGA-TPGS nanoparticles (HPTNs) were prepared used PLGA-TPGS as the carrier material. It was because of the difference in the solubility profile of the 2 drugs. What's more, as the proportion of drugs in the compound preparations has a great impact on efficacy, the two drugs were incorporated into NPs first, and the NPs were then united before use. This method ensures that the dosage and proportion of EMO and HS are targeted to the liver simultaneously, and the best combined dosages and proportions of two drugs were identified through *in vitro* cytotoxicity and apoptosis assays. In addition, to illustrate that the combination of EPTNs and HPTNs can achieve the synergistic inhibition of liver cancer, we investigated the *in vivo* therapeutic effects on the primary hepatocarcinogenic mouse model induced by diethylnitrosamine (DEN).

MATERIALS AND METHODS

Materials

EMO, TPGS, ethyl acetate, sodium dodecyl sulphate (SDS, purity 99%), coumarin-6 (C6, purity 99%), fluorescein, and eosin were purchased from Sigma-Aldrich (St. Louis, MO, USA). HS (160 IU/mg) was purchased from the National Institute for the Control of Pharmaceutical and Biological Products (Beijing, China). PLGA-TPGS (M_w : 21–22 kD) was synthesized and contributed by Dr. Lin Mei, who works at the Academy of Life Sciences, Tsinghua University (Beijing,

China). HepG2 cells were purchased from the Chinese Academy of Medical Sciences Cell Centre. HCa-F cells were provided by the Morphological Lab of Dalian Medical University (Dalian, China). 4,6-Diamidino-2-phenylindole dihydrochloride (DAPI) was obtained from Fluka (Buche, Switzerland). 4-[3-(4-iodophenyl)-2-(4-nitrophenyl)-2H-5-tetrazolio]-1,3-benzene sulphonate (WST-1) was purchased from Roche Applied Sciences (Basel, Switzerland). Methanol, acetic acid, and acetonitrile were purchased from Tedia (HPLC grade; Fairfield, OH, USA). All other chemicals and reagents were commercially available and of the highest quality.

Preparation of EMO-Loaded NPs and HS-Loaded NPs

The EPTNs were prepared using an ultrasonic emulsification-solvent evaporation method (15). In brief, the organic phase of 8 mL ethyl acetate in which a given amount of EMO and 100 mg PLGA-TPGS copolymer were dissolved was dropped slowly into 120 mL of a 0.03% purified aqueous solution of TPGS while being sonicated for 2 min at 100 W (transmit frequency) in an ice bath. Then, the prepared emulsions were stirred constantly overnight at 400 r/min in the ice bath at room temperature to remove ethyl acetate. The NPs were collected by centrifuging at 20,000 r/min for 15 min in a high-speed refrigerated centrifuge (Sorvall Evolution RC, Kendro Laboratory Products, Asheville, NC, USA) and washed 3 times with deionized water to remove the unloaded drug and materials. Finally, the NPs were dispersed in 5 mL deionized water and then freeze-dried for 24 h for further use. Similarly, EMO/C6-loaded PLGA-TPGS NPs (ECPTNs) were prepared in the same way except that EMO, C6, and PLGA-TPGS copolymer were dissolved in ethyl acetate at the same time. Blank PLGA-TPGS NPs (BPTNs) without any drug were also prepared in the same way.

The HPTNs were also prepared by ultrasonic emulsification-solvent evaporation. One millilitre deionized water solution, which included a certain amount of HS, was dropped slowly into 8 mL ethyl acetate containing 100 mg of PLGA-TPGS copolymer and sonicated at 200 W in an ice bath to form W/O emulsions. The emulsions were poured into 120 mL 0.03% TPGS aqueous solution to form W/O/W multiple emulsions while being sonicated at 100 W for 12 min. Then, the prepared W/O/W multiple emulsions were stirred continuously overnight at 400 r/min in the ice bath at room temperature to remove ethyl acetate. Then, the NPs were preserved as indicated previously. In addition, HS/eosin-loaded PLGA-TPGS NPs (HEPTNs) and HS/fluorescein-loaded PLGA-TPGS NPs (HFPTNs) were prepared using the method described above with the simultaneous addition of a certain amount of HS, eosin, or fluorescein dissolved in deionized water. All types of NPs were

prepared six times in parallel using the same methods described above, and all NPs were characterized.

Characterization of NPs

Size, Size Distribution, ζ -Potential, and Morphology

The particle size, including the size distribution and ζ -potential of NPs, were measured, respectively, using NanoZS90 Light Scattering and Laser Doppler Anemometry (Zetasizer Nano ZS90, Malvern Instruments Ltd., Malvern, UK). Before measurement, approximately 2 mg of freeze-dried NPs were dispersed in 3 mL deionized water. All data were acquired from six averaged samples. The surface morphology of NPs was imaged using a transmission electron microscope (TEM, testing conditions: accelerating voltage, 120.0 kV; JEM-2000EX, Japan Electron Optics Laboratory Co., Ltd, Tokyo, Japan). A small quantity of NP suspensions was placed on a copper grid surface for a period of time. One drop of 2.5% phosphotungstic acid was added to the surface for 3 min after residual fluid was removed, and the copper grid was air dried at room temperature. Then, the samples were observed using TEM.

Drug Loading, Encapsulation Efficiency, and *in Vitro* Drug Release

The drug loading (DL) and encapsulation efficiency (EE) of EPTNs and HPTNs were detected by RP-HPLC (1260 Series, Agilent Technologies, Santa Clara, CA, USA). To study the cellular uptake of ECPTNs and HEPTNs quantitatively, we also measured the DL and EE of C6 and eosin by RP-HPLC. The full methods can be found in the [Supplementary materials](#).

$$DL(\%) = \frac{\text{Weight of drug-loaded in the NPs}}{\text{Weight of the NPs}} \times 100 \quad (1)$$

$$EE(\%) = \frac{\text{Weight of drug-loaded in the NPs}}{\text{Weight of the total drug}} \times 100 \quad (2)$$

The *in vitro* release of EMO from the EPTNs and ECPTNs and HS from the HPTNs, HEPTNs, and HFPTNs were also evaluated using the dialysis method (15) as shown in the [Supplementary materials](#).

Cellular Uptake of NPs

In this paper, HepG2 cells and HCa-F cells were cultured in high glucose Dulbecco's modified Eagle's medium (HDMEM, Thermo Fisher Scientific, Waltham, MA, USA) supplemented with 10% heat-inactivated fetal bovine serum (FBS, Thermo Fisher Scientific) and 1% antibiotics. The cultures were maintained in 5% CO₂ at 37°C. Before using HCa-F cells for cellular uptake, the number of live HCa-F

cells was computed and adjusted to 3.0×10^7 cells/mL. Six-week-old male mice weighing approximately 20–22 g were obtained from the Dalian Medical University Laboratory Animal Centre and were intraperitoneally injected with 200 μ L HCa-F cells; ascites could be extracted under sterile conditions approximately 7 days later. The concentration of ascites cell suspensions was adjusted to $2.0\text{--}2.3 \times 10^7$ cells/mL with PBS and then incubated with HEPTNs (the concentration of eosin in HEPTNs was 200.0 μ g/mL, and the concentration of HS was 147.3 μ g/mL) and ECPTNs (the concentration of C6 in ECPTNs was 200.0 μ g/mL, and the concentration of EMO was 202.5 μ g/mL) at 37°C for 4 h. The cells were rinsed with cold PBS three times and then fixed with 75% ethanol (kept at -20°C) for 10 min. Finally, the cells were stained with DAPI for 15 min and washed three times with PBS. Because HCa-F cells are suspension cells, they were centrifuged at 1000 r/min for 5 min each time, but HepG2 cells did not require this step. The cellular uptake of NPs was recorded using a confocal laser scanning microscope (CLSM) (TCS SP5, Leica Microsystems Co. Ltd., Solms, Germany). The CLSM images of HEPTNs, ECPTNs, and the nuclei of the cells stained by DAPI were determined with the differential interference contrast (DIC) channel, the blue channel (DAPI) with excitation at 340 nm, the green channel (C6) with excitation at 488 nm, and the red channel (eosin) with excitation at 632 nm.

After observation, two different cells in the orifice plate were collected and dispersed in purified water for quantitative studies, and the full methods used for these analyses are described in the [Supplementary materials](#). Cellular uptake efficiency was calculated by the ratio of the measured quantity of drugs and probes in cells to the added amount.

In Vitro Cytotoxic Combination Effect and Cell Apoptosis

In our previous paper (15), EPTNs were prepared and investigated quantitatively in an *in vitro* cytotoxicity experiment, and the results indicated that the best concentration of EMO was 40 μ g/mL (these procedures can be viewed in the [Supplementary materials](#)); therefore, in our present study, 40 μ g/mL was also used as the concentration of EMO in the EPTNs, and the full methods used for these procedures are also described in the [Supplementary materials](#). Meanwhile, 5-Fluorouracil was used as a negative control drug because it is a chemotherapy drug commonly used to treat the transhepatic arterial chemotherapy and embolization (TACE), and it can be injected *via* an intravenous route, which coincided with the delivery method chosen for the NPs. The combination effect was defined with the following equation:

$$Q = \frac{E_{(A+B)}}{E_A + E_B - E_A \times E_B} \quad (3)$$

$E_{(A+B)}$, which indicates the joint inhibitory rate of EPTNs combined with HPTNs or EMS combined with HSS. E_A and E_B represented the inhibition rate of EPTNs and HPTNs or EMS and HSS, respectively. $Q > 1.15$ means that the combination of two NPs (or solutions) had synergistic effects (++). Q between 0.85 and 1.15 indicated that the combination of two NPs (or solutions) had additive effects (+). However, if Q was 0.55–0.85, the combination of two NPs (or solutions) had antagonistic effects (-), which were more apparent if $Q < 0.55$ (23).

HepG2 cell apoptosis was detected according to the instructions of the Annexin V-fluorescein isothiocyanate (FITC) cell apoptosis detection kit (Life Technologies, Carlsbad, CA, USA) and assessed by flow cytometry; the full methods used for these procedures are described in the [Supplementary materials](#).

In Vivo Drug Concentrations of ECPTNs and HFPTNs and Frozen Slices for Evaluating Liver Targeting Properties

Establishment of Animal Model and Analysis of Biological Samples

All animal experimentation was in accordance with the guidelines set by the Institutional Animal Care and Use Committee (IACUC) (Dalian Medical University, Dalian, China). Six-week-old Kunming male mice (Specific Pathogen Free grade, approximately 20–22 g) were obtained from the Dalian Medical University Laboratory Animal Centre and divided randomly into 2 groups (the experimental group and control group). The mice did not fast before the experiment and all received the standard laboratory diet. Four mice were fed separately in one cage and maintained in a room with a constant temperature ($22 \pm 1^\circ\text{C}$), humidity of 75% and a dark–light cycle (12 h/12 h). The experimental group was used to establish the primary hepatocarcinogenic mouse model induced by DEN (24) as described in the [Supplementary materials](#).

The methods used to process the biological samples to determine the EMO and HS content in the blood samples and different organs are also described in the [Supplementary materials](#).

Administration of Drugs

Three mice were selected randomly from the experimental group as the blank control group and euthanized immediately after other mice were administered drugs. The organs (liver, heart, spleen, lungs, and kidneys) of three mice were isolated immediately and kept at -80°C for 20 min. The rest of the mice in the experimental group were selected randomly and divided into 2 groups (NPs group and Solutions group), which

were administered therapeutics by tail vena injection. In the NPs group, a total of 64 mice were injected with ECPTN and HFPTN suspensions (dispersed evenly with normal saline solution containing 20% PEG400 by sonicating at 100 W for 2 min in ice water) at 6 mg EMO/kg and 2000 IU HS/kg (containing approximately 5.92 mg/kg C6 and 14.61 mg/kg FR in total) according to mouse weights. In the Solutions group, a total of 48 mice were injected with EMO combined with HS solutions (EM&HSS, normal saline containing 20% PEG400 as solvent) according to weight at the same doses above. After injection, blood samples were obtained from the cardiac apical site, and the organs (liver, heart, spleen, lungs and kidneys) were separated immediately after six mice of each group were anesthetized by ether inhalation after 0.08 (*i.e.*, 5 min), 0.5, 1, 2, 4, 8, 12, and 24 h. The treatment and analysis of the blood samples and organs were performed as mentioned above. For a fluorescence imaging study with frozen slices, three mice from the NPs group (total 18 mice) were executed at the timepoints of 0.5, 1, 2, 4, 8 and 12 h, and the organs (liver, heart, spleen, lungs and kidneys) of each mouse were isolated and transferred immediately to -80°C for 20 min. The frozen slices were prepared using a frozen microtome (HM500, Microm International GmbH, Walldorf, Germany). A total of 10 pieces with approximate 7 μm thickness were obtained from each frozen organ. The frozen slices were observed using a fluorescence inversion microscope (FIM) (Olympus IX81; Olympus Corporation, Tokyo, Japan).

The liver targeting of ECPTNs and HFPTNs in the liver were determined comprehensively using the following detection indicators: (1) Targeting index (TI) and selectivity index (SI): TI refers to the drug concentration ratio of drug-loaded NPs (T) to free drug (S), respectively ($\text{TI} = C_T/C_S$), and SI refers to the ratio of targeting organ (liver) drug concentration to non-target organ drug concentration ($\text{SI} = C_{\text{liver}}/C_{\text{non-targeting organ}}$); (2) Relative targeting efficiency (Re) and targeting efficiency (Te): the areas under concentration-time curve ($\text{AUC}_{0-24\text{ h}}$) of EMO and HS in the plasma and organs were measured by the trapezoidal method. Re refers to the ratio of AUC in each organ between drug-loaded NPs (T) and free drug solutions (S), respectively ($\text{Re} = \text{AUC}_T/\text{AUC}_S$). Te refers to the ratio of AUC between the targeting organ and non-targeting organ ($\text{Te} = \text{AUC}_{\text{liver}}/\text{AUC}_{\text{non-targeting organ}}$) (25).

In Vivo Therapeutic Efficacy

Eighty six-week-old Kunming male mice (20–22 g) were selected as the experimental group to establish the primary hepatocarcinogenic mouse model induced by DEN and CCl_4 using the method mentioned above. At the same time, eight mice were used as the normal control group without any drug treatment. After 20 weeks, three mice in the experimental group were selected randomly to assess tumour

establishment, and the other mice were divided randomly into nine test groups (each group has 8 animals) according to the following scheme: Group A, the blank control group (20% v/v PEG400-normal saline solutions); Group B, BPTN (BPTN suspensions) group; Group C, fluorouracil solution (FS, commercial fluorouracil for injection solutions) group; Group D, EMO solution (EMS) group; Group E, HS solution (HSS) group; Group F, EMO&HSS group; Group G, EPTN (EPTN suspension) group; Group H, HPTN (HPTN suspension) group; Group I, EPTN&HPTN (OPTN combined with HPTN suspension) group. Twenty percent (v/v) PEG400-normal saline solution was used as solvent for the FS, EMS, HSS, and EM&HSS groups. All NPs including BPTNs, EPTNs, HPTNs and EPTNs&HPTNs were dispersed into 20% (v/v) PEG400-normal saline solution and sonicated at 100 W for 1 min in an ice bath to form suspensions, respectively. The mice in Groups D and G were administered doses equivalent to 6 mg/kg EMO, whereas Group C was administered equivalent 6 mg/kg fluorouracil. The mice in Groups E and H were administered 2000 IU/kg equivalent HS. The mice in Groups F and I were administered 6 mg/kg and 2000 IU/kg equivalent EMO and HS, respectively. The mice in Group B were administered with the same PLGA-TPGS concentration as EPTN, 21.82 mg/kg. The mice were dosed by tail vena injection once every 3 days for a sequential 30 days and were given normal food and water daily. After 30 days, the blood samples were obtained from the cardiac apical site of each mouse after they were anesthetized (inhalation of ether), and the samples were centrifuged at 3000 r/min for 10 min to obtain serum. Liver functional indexes such as γ -glutamyltransferase (γ -GT), alanine aminotransferase (ALT), aspartate aminotransferase (AST), albumin (ALB), and total bilirubin (T-BIL), were examined in serum using a 7060 automatic clinical biochemical analyzer (HITACHI, Tokyo, Japan). These mice were sacrificed by cervical dislocation, and livers were isolated after blood was obtained; approximately 0.5 g liver from each mouse was combined with 9-fold volumes of normal saline to prepare the tissue homogenates, which were centrifuged at 2500 r/min for 10 min. Then, the liquid supernatant was used for the measurement of γ -GT, ALT, AST and total proteins (TP) in the liver. The residual liver in each mouse was prepared as formalin-fixed, paraffin-embedded sections for H&E staining and the thickness of the slices was 5 μ m, which were observed using an optical microscope (DM400 B, Leica, Heidelberg, Germany).

Statistical Analysis

The results are presented as the means \pm sd. Statistical comparisons were made by Student's *t*-test (SPSS13.0 statistical software, International Business Machines Corporation, Armonk, NY, USA). The accepted level of significance was $p < 0.05$.

RESULTS

Characterization of NPs

The TEM images of EPTNs, ECPTNs, HPTNs, HFPTNs and HEPTNs are shown in Fig. 1a. TEM reveals that these NPs were all spherical and regular, and all had a mean diameter in the range of 100–200 nm, which was consistent with the results of particle size listed in Table I measured by NanoZS90 Light Scattering. The size, size distribution, and ζ -potential of EPTNs, ECPTNs, HPTNs, HFPTNs and HEPTNs are listed in Table I. The mean particle size of EPTNs and ECPTNs was 144.8 ± 1.6 nm and 162.6 ± 1.5 nm with a much narrower polydispersity index (PDI); both were smaller than HS-loaded NPs (>170 nm, also shown in Fig. 1b). As also listed in Table I, the absolute values of ζ -potential for five NPs were all above 23 mV.

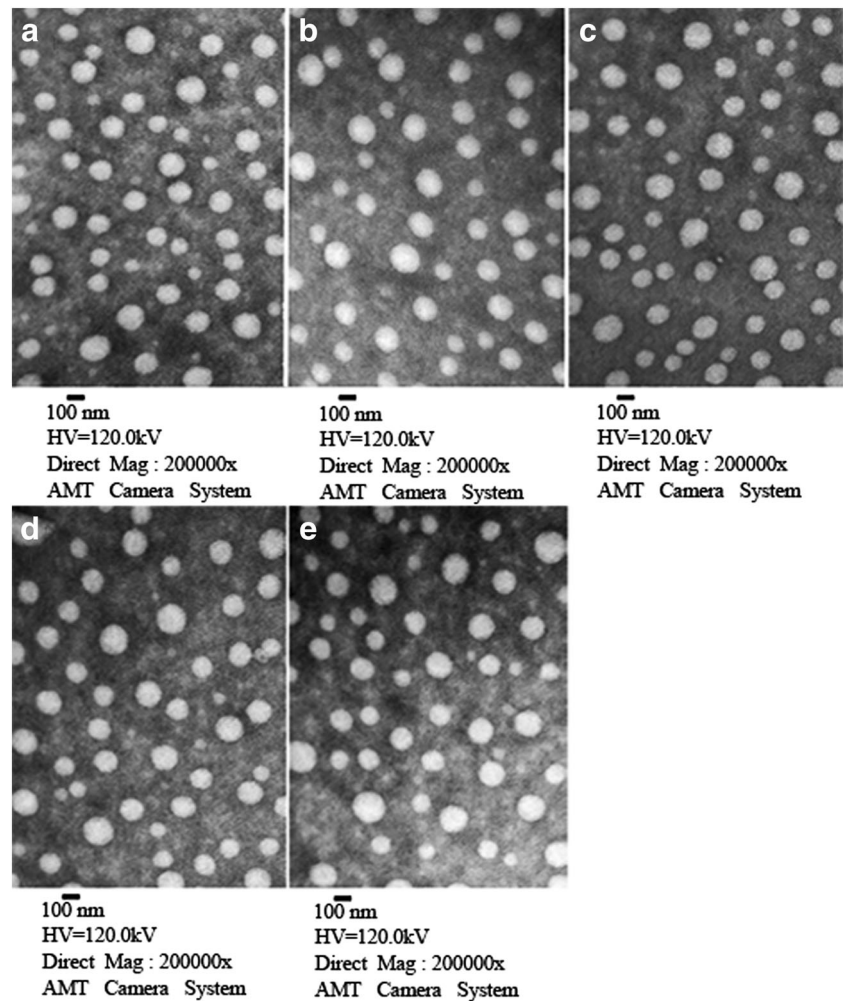
The DL and EE of EPTNs are $21.9 \pm 1.4\%$ and $92.8 \pm 1.5\%$, and the DL and EE of HPTNs are $12.4 \pm 1.7\%$ and $53.5 \pm 1.4\%$, respectively (also listed in Table I). Because HS is a water-soluble compound with higher molecular weight that makes it difficult to prepare NPs, the DL and EE of HPTNs are lower than those of EPTNs. Moreover, the DL of EMO in ECPTNs was only $10.4 \pm 1.4\%$, similar to that of HS in HFPTNs or HEPTNs, because the amount of EMO is half that of EPTN in the preparation process. The EEs of EPTNs and ECPTNs were almost the same (greater than 85%); both were much higher than that of HS-loaded NPs, which was approximately 50%.

The *in vitro* drug release profiles of NPs are shown in Fig. 2. The release process for EMO is illustrated in Fig. 2a. The release trends of EPTNs and ECPTNs were consistent with that of HPTNs. For example, an initial burst of EPTN (30.6%) release was observed on the first day, and then the stable diffusion stage continued until the 9th day, when the cumulative drug release of NPs was greater than 70%; more than 85% of EMO was released from NPs at the 30th day. *In vitro* drug release models of HPTNs, HEPTNs, and HFPTNs indicated a biphasic release with an initial burst effect followed by a slow release. However, HS had released completely in the first day (99.8%), whereas the release rate of HPTNs was 28.7%. As shown in Fig. 2b, the release of HPTNs, HEPTNs, and HFPTNs was in the stable diffusion stage after 9 days (71.3, 67.9, and 65.1%). After 30 days, the release of HPTNs, HEPTNs, and HFPTNs were more than 85% (91.2, 88.9, and 87.8%).

Cellular Uptake of NPs

The CLSM images (Fig. 3) show that the red fluorescence of HEPTNs (red channel) and the green fluorescence of ECPTNs (green channel) were both closely localized around the nuclei (blue, stained by DAPI), which indicated that

Fig. 1 Characterization images of drug-loaded nanoparticles. a, b, c, d, and e are TEM images of EMO-loaded PLGA-TPGS nanoparticles (EPTNs), EMO/C6-loaded PLGA-TPGS nanoparticles (ECPTNs), HS-loaded PLGA-TPGS nanoparticles (HPTNs), HS/eosin-loaded PLGA-TPGS nanoparticles (HEPTNs), and HS/fluorescein-loaded PLGA-TPGS nanoparticles (HFPTNs) (200,000 \times), respectively.



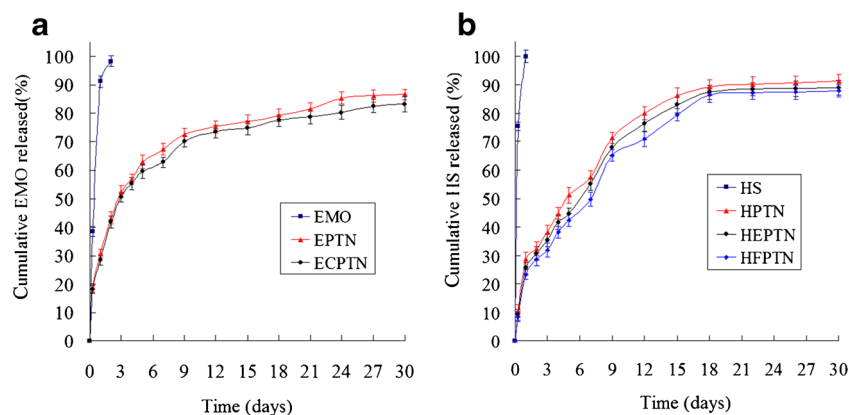
HEPTNs and ECPTNs had been internalized into the cells simultaneously, and the results of HepG2 cells and HCa-F cells were consistent. For the quantitative study, the concentrations of C6 and EMO were $120.9 \pm 1.9 \mu\text{g/mL}$ and $124.3 \pm 2.0 \mu\text{g/mL}$ ($n = 6$), and the cellular uptake efficiencies of C6 and EMO were 60.4 and 61.4%, respectively, in HepG2 cells. Furthermore, the concentrations of eosin and HS were $118.2 \pm 1.8 \mu\text{g/mL}$ and $88.7 \pm 1.4 \mu\text{g/mL}$ ($n = 6$), and the cellular uptake efficiencies of eosin and HS

were 59.1 and 60.2%, respectively, in HepG2 cells. Similarly, in HCa-F cells, the concentrations of C6 and EMO were $96.1 \pm 1.7 \mu\text{g/mL}$ and $97.2 \pm 1.6 \mu\text{g/mL}$ ($n = 6$), and the cellular uptake efficiencies of C6 and EMO were 48.1 and 48.0%, respectively. Moreover, the concentrations of eosin and HS were $93.7 \pm 1.6 \mu\text{g/mL}$ and $69.8 \pm 1.4 \mu\text{g/mL}$ ($n = 6$), and the cellular uptake efficiencies of HS and eosin were 46.9 and 47.4%, respectively, in HCa-F cells.

Table 1 Characterization of NPs. ($n = 6$, mean \pm SD)

Sample	Size (nm)	PDI	ζ -potential (mV)	DL (%)	EE (%)
EPTNs	148.3 ± 1.6	0.087 ± 0.019	-23.5 ± 1.7	21.9 ± 1.4 (EMO)	92.8 ± 1.5 (EMO)
ECPTNs	162.6 ± 1.5	0.124 ± 0.021	-23.2 ± 1.8	10.4 ± 1.4 (EMO) 10.3 ± 1.7 (C6)	89.9 ± 1.9 (EMO) 86.5 ± 1.6 (C6)
HPTNs	178.1 ± 1.8	0.098 ± 0.025	-23.1 ± 1.5	12.4 ± 1.7 (HS)	53.5 ± 1.4 (HS)
HEPTNs	186.5 ± 1.4	0.183 ± 0.024	-22.8 ± 1.1	6.4 ± 1.8 (HS) 8.6 ± 1.4 (eosin)	54.6 ± 1.9 (HS) 74.1 ± 1.3 (eosin)
HFPTNs	190.7 ± 1.9	0.135 ± 0.023	-23.5 ± 1.6	6.7 ± 1.5 (HS) 7.8 ± 1.8 (FR)	57.7 ± 1.6 (HS) 67.4 ± 1.3 (FR)

Fig. 2 a is *in vitro* drug release profiles of EMO, EMO-loaded PLGA-TPGS nanoparticles (EPTNs), EMO/C6-loaded PLGA-TPGS nanoparticles (ECPTNs), b is *in vitro* drug release profiles of HS, HS-loaded PLGA-TPGS nanoparticles (HPTNs), HS/eosin-loaded PLGA-TPGS nanoparticles (HEPTNs), and HS/fluorescein-loaded PLGA-TPGS nanoparticles (HFPTNs). All release data represent the mean \pm SD of sextuplicate experiments.



In Vitro Cytotoxic Combination Effect and Cell Apoptosis

As listed in Table II, the inhibition ratio (IR) of EMO (40 μ g/mL) combined with HS at the various concentrations was further increased compared with EMO administered alone. In particular, the IR of EPTNs combined with HPTNs was more significant than that of EMS combined with HSS. For example, the IR of EPTNs increased from 56.27 to 87.84% when 40 μ g/mL EPTNs was combined with 20 IU/mL HPTNs, and Q was 1.30, which indicated synergistic effects (++) . Meanwhile, the IR of EMS increased from 38.69 to 49.75% when 40 μ g/mL EMS was combined with 20 IU/mL HSS, and Q was 1.12, which indicated additive effects (+). Thus, 40 μ g/mL EPTNs combined with 20 IU/mL HPTNs had more synergistic effects; therefore, it was used as the best concentration and ratio of EMO combined with HS for *in vivo* liver targeting and pharmacodynamics studies.

The results of Annexin-PI double staining flow cytometry are listed in Table III. The EPTN&HPTN group at concentrations of 40 μ g/mL and 20 IU/mL, respectively, achieved the highest apoptotic rate among these groups, and the apoptotic cells increased gradually with increasing concentrations.

The cell apoptosis and necrosis in the negative control group were very low, and there was a significant difference between the EPTN&HPTN group and the FS positive control group ($p < 0.01$). Moreover, the apoptotic rate of the EMS group was 33.2%, which increased by 7.7% upon combination with HS. At the same time, the apoptotic rate of the EPTN group was 57.3%, which increased by 24.8% upon combination with HPTNs. HepG2 cells showed altered histomorphology, including decreased volume, cell detachment, and the accumulation of chromosomes, which indicated typical apoptotic morphological transformation.

In Vivo Drug Concentration and Frozen Liver Slices for Evaluating Liver Targeting Capacity of ECPTNs and HFPTNs

Drug Concentrations in Biological Samples at Designated Timepoints and Detection Indexes for Evaluating the Liver Targeting Capacity of ECPTNs and HFPTNs in Mice

The concentrations of EMO and HS in the plasma and different organs of Group A and Group B mice were measured by HPLC

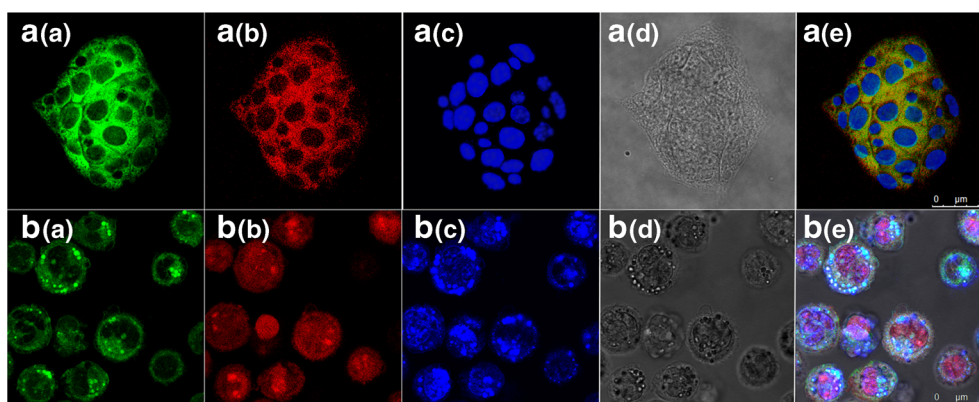


Fig. 3 The confocal laser scanning microscope (CLSM) images (400 \times) of HepG2 cells and HCa-F cells after 24 h incubation with NPs suspensions. ECPTNs and HEPTNs were green and red while nuclei of the cells were blue stained using DAPI. a(a) and b(a) are green fluorescence field images of ECPTNs and HEPTNs uptaken by HepG2 cells and HCa-F cells; a(b) and b(b) are red fluorescence field images of ECPTNs and HEPTNs uptaken by HepG2 cells and HCa-F cells; a(c) and b(c) are blue fluorescence field images of HepG2 and HCa-F cell nuclei dyed by DAPI; a(d) and b(d) are bright field images of HepG2 cells and HCa-F cells; a(e) is a combined image of a(a), a(b), and a(c), and b(e) is a combined image of b(a), b(b), and b(c), respectively.

Table II Results of the Synergistic Anticancer Effect of EPTNs Combined with HPTNs and EMS Combined with HSS ($n = 6$)

Dose		Inhibition ratio (%, $\bar{X} \pm s$)	Q	Combination effect	Dose		Inhibition ratio (%, $\bar{X} \pm s$)	Q	combination effect
EPTNs ($\mu\text{g/mL}$)	HPTNs (IU/mL)				EMS ($\mu\text{g/mL}$)	HSS (IU/mL)			
40	0	56.27 \pm 0.26			40	0	38.69 \pm 0.24		
0	2.5	9.09 \pm 0.25			0	2.5	3.37 \pm 0.25		
0	5	14.57 \pm 0.27			0	5	5.06 \pm 0.28		
0	10	19.48 \pm 0.23			0	10	8.25 \pm 0.22		
0	20	26.11 \pm 0.21			0	20	9.18 \pm 0.21		
0	40	33.36 \pm 0.29			0	40	10.24 \pm 0.23		
40	2.5	61.72 \pm 0.24	1.02	+	40	2.5	40.52 \pm 0.20	0.99	
40	5	69.67 \pm 0.20	1.11	+	40	5	43.37 \pm 0.19	1.04	+
40	10	78.25 \pm 0.22	1.21	++	40	10	46.51 \pm 0.23	1.06	+
40	20	87.84 \pm 0.28	1.30	++	40	20	49.75 \pm 0.26	1.12	+
40	40	89.63 \pm 0.21	1.26	++	40	40	50.08 \pm 0.23	1.11	+

The symbol of ++ means that the combination of two NPs (or solutions) had synergistic effects ($Q > 1.15$). The symbol of + indicated that the combination of two NPs (or solutions) had additive effects (Q between 0.85 and 1.15)

after tail-intravenous administration. As shown in Fig. 4a(a) and b(a), the concentrations of EMO and HS reached maxima after 1 h of injection, which indicated that the two drugs could be targeted to the liver at the same time. The drugs were released slowly over 8 h into the plasma and over 24 h into the liver of the mice. As shown in Fig. 4a(b) and b(b), EMO and HS could not be detected after approximately 8 h in the plasma and liver after injecting EMS combined with HSS. This finding illustrated that ECPTNs and HFPTNs could effectively prolong the retention time of EMO and HS in the plasma and liver and significantly increase the concentration of the two drugs in the liver.

In Tables IV and V, the detection indicators (TI, SI, Re, and Te) were used to measure the liver targeting of the two drugs. As listed in Table IV, TI and SI were greater than 1.0, with the exception of the TI_{HS} and SI in plasma at 0.08 h. This finding illustrated that ECPTNs and HFPTNs had good liver targeting

Table III Effect on Apoptosis of HepG2 Cells Induced by Different Drug After 24 h ($n = 6$, mean \pm SD)

Group	Cell ratio (%)		
	Survival cells	Apoptotic cells	Necrotic cells
negative control	98.1 \pm 1.2	0.8 \pm 0.8	1.1 \pm 1.2
FS	58.3 \pm 1.9	15.6 \pm 1.5	26.1 \pm 1.8
EMS	62.4 \pm 2.3	33.2 \pm 1.7 ^c	4.4 \pm 1.0
HSS	90.7 \pm 2.1	5.4 \pm 1.3 ^c	3.9 \pm 1.5
EM&HSS	50.9 \pm 1.5	40.9 \pm 2.0	8.2 \pm 1.3
EPTN	39.0 \pm 1.7 ^{ad}	57.3 \pm 2.4 ^{ad}	3.7 \pm 1.4
HPTN	66.5 \pm 2.5	14.7 \pm 1.2	19.8 \pm 1.6
EPTN&HPTN	10.6 \pm 1.4 ^{bd}	82.1 \pm 2.6 ^{bd}	7.3 \pm 2.1

^a $p < 0.05$, ^b $p < 0.01$ versus corresponding EMS group; ^c $p < 0.05$, ^d $p < 0.01$ versus corresponding FS group

capacity at different timepoints. Table V shows that the Re_{EMO} and Re_{HS} of the liver were the largest, which further indicated that ECPTNs and HFPTNs had improved liver-targeting capacity. As also observed in Table V, the Te of ECPTNs and HFPTNs were greater than 3.0, which further showed that ECPTNs and HFPTNs had good liver-targeting capacity.

Fluorescence Imaging Study of Frozen Slices for Evaluating the Liver-Targeting Capacity of ECPTNs and HFPTNs in Mice

The FIM images (200 \times) of frozen organ slices at the timepoints of 0.5, 1, 2, 4, 8, and 12 h are shown in Fig. 5 and Figures S2-S5. The yellow green fluorescence of ECPTNs and HFPTNs (green channel) accumulated most in the liver, followed by the lungs and spleen and then by the heart and kidneys. This finding indicated that ECPTNs and HFPTNs not only had a good effect on the liver but also reduced the toxicity of the drugs to the heart and kidneys. Meanwhile, the distribution of NPs was greatest and the fluorescence was strongest in all of organs after 1 h compared with 0.5, 2, 4, 8, and 12 h. These results are consistent with the AUC and C_{max} *in vivo* targeting evaluation indicators of ECPTNs and HFPTNs.

In Vivo Therapeutic Effect Study

The results of liver function experiments are listed in Table VI. Compared with the normal control group, the liver functional indexes including γ -GT, ALT, AST, and T-BIL in serum and γ -GT, ALT, and AST in the liver were significantly increased ($p < 0.05$, $p < 0.01$) in nine experimental groups. For example, the γ -GT for the EPTN&HPTN group was only increased by 3.7 U/L, and that for the EM&HSS group was increased by 9.0 U/L ($p < 0.05$). However, the γ -GT for the

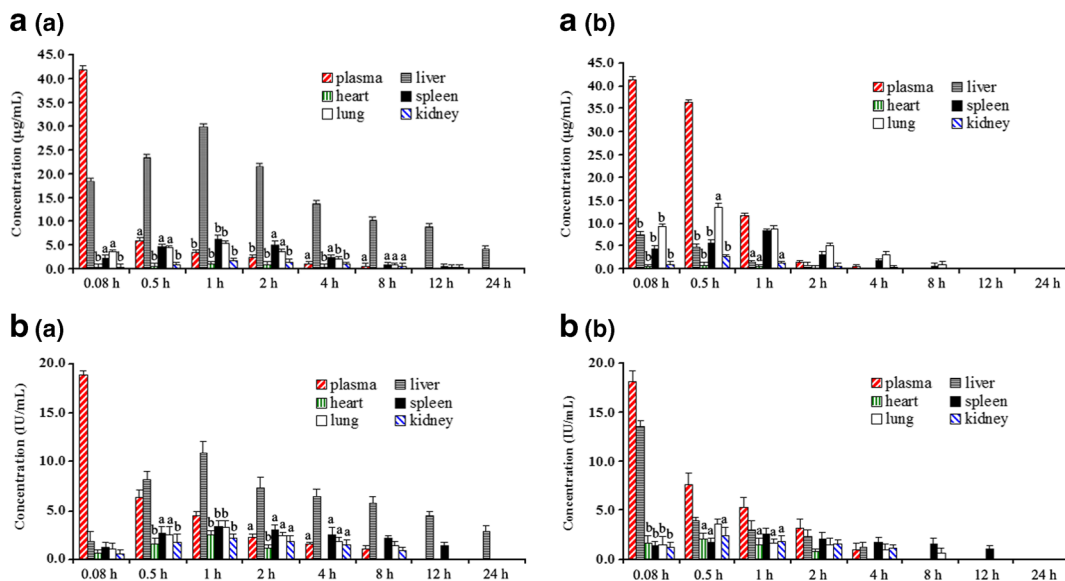


Fig. 4 The EMO and HS concentration-time column shape images in different groups ($n = 8$, mean \pm SD). a(a) and b(a) are the concentration-time column shape images of EMO/C6-loaded PLGA-TPGS nanoparticles (ECPTNs) and HS/fluorescein-loaded PLGA-TPGS nanoparticles (HFPTNs) in plasma and different organs of the mice after being injected ECPTN combined with HFPTN suspensions *via* tail vena, ^a $p < 0.05$, ^b $p < 0.01$ versus corresponding liver; a(b) and b(b) are the concentration-time column shape images of EMO and HS solutions in plasma and different organs of the mice after being injected EMO combined with HS solutions *via* tail vena, respectively. ^a $p < 0.05$, ^b $p < 0.01$ versus corresponding plasma. All data represent the mean \pm SD of experiments in octuplicate.

blank control group was increased by 12.9 U/L ($p < 0.01$). Meanwhile, the ALT and AST for the EPTN&HPTN group were only increased by 29.1 and 30 U/L, and that for the EM&HSS group was increased by 57.2 and 87.6 U/L ($p < 0.05$); however, the ALT and AST for the blank control group were increased by 68.0 and 96.7 U/L ($p < 0.01$). Furthermore, the ALB and TP were significantly decreased in the serum for the nine experimental groups ($p < 0.05$, $p < 0.01$) compared to the normal control group. The results (except for ALB and T-BIL) in the liver were consistent with those in serum. The body weight of each mouse in the experimental group except for the blank control and BPTN groups was a certain extent increased in the period of drug administration (as shown in Figure S6). At the beginning of 7th days, the growth rate of body weight of each mouse in the EPTN&HPTN group was relatively fast compared to the blank control and BPTN groups. However, there was no significant difference compared to the other experimental groups.

Figure 6 presents the morphology of parts of the livers of each group. The livers of each mouse except those of the normal control group showed hard, gray nodules varying in size from 5 to 12 mm. The typical H&E staining images are shown in Fig. 7. The internal structure, cell differentiation, cell nucleus, and cytoplasm of lesions were observed with an optical microscope. According to the Edmonson-Steiner classification method (26), the results were divided into Grade I through Grade IV. Grade I indicated eosinophilic staining; tumour cells were similar to normal liver cells, and cytoplasm was abundant. In Grade II, cancer cells had abundant cytoplasm; there was increased eosinophilic staining, irregular shape, and a slightly larger nucleus. Grade III was assigned for basophilic staining; the shape of cancer cells was polymorphic, and the nuclei were large and irregular. Moreover, giant tumour cells began to appear. Grade IV had obviously polymorphic cancer cells arranged loosely and without structure. Furthermore, there were also increased levels of giant tumour

Table IV TI and SI Values of EMO and HS in Mice at Different Timepoints After Tail-Intravenous Injection

Index	Time (hours)							
	0.08	0.5	1	2	4	8	12	24
TI _{EMO}	2.4	4.9	19.9	27.0	27.4	20.4	17.8	8.6
SI _{EMO-plasma}	0.4	4.0	8.5	9.0	12.5	14.6	–	–
TI _{HS}	0.1	2.1	3.5	3.0	4.9	9.5	7.5	4.8
SI _{HS-plasma}	0.1	1.3	2.4	3.2	4.0	5.2	–	–

Table V Te and Re Values of EMO and HS in Plasma and Different Organs

Index	Plasma	Liver	Heart	Spleen	Lung	Kidney
Re _{EMO}	0.6	38.9	2.5	1.3	0.7	2.8
Re _{HS}	1.2	7.7	1.3	1.4	1.7	1.5
Te _{ECPTN}	9.8	–	65.5	8.1	9.5	19.0
Te _{EMS}	0.2	–	4.3	0.3	0.2	1.4
Te _{HFPTN}	6.2	–	22.0	3.1	6.3	8.7
Te _{HSS}	0.6	–	4.1	0.5	1.5	1.7

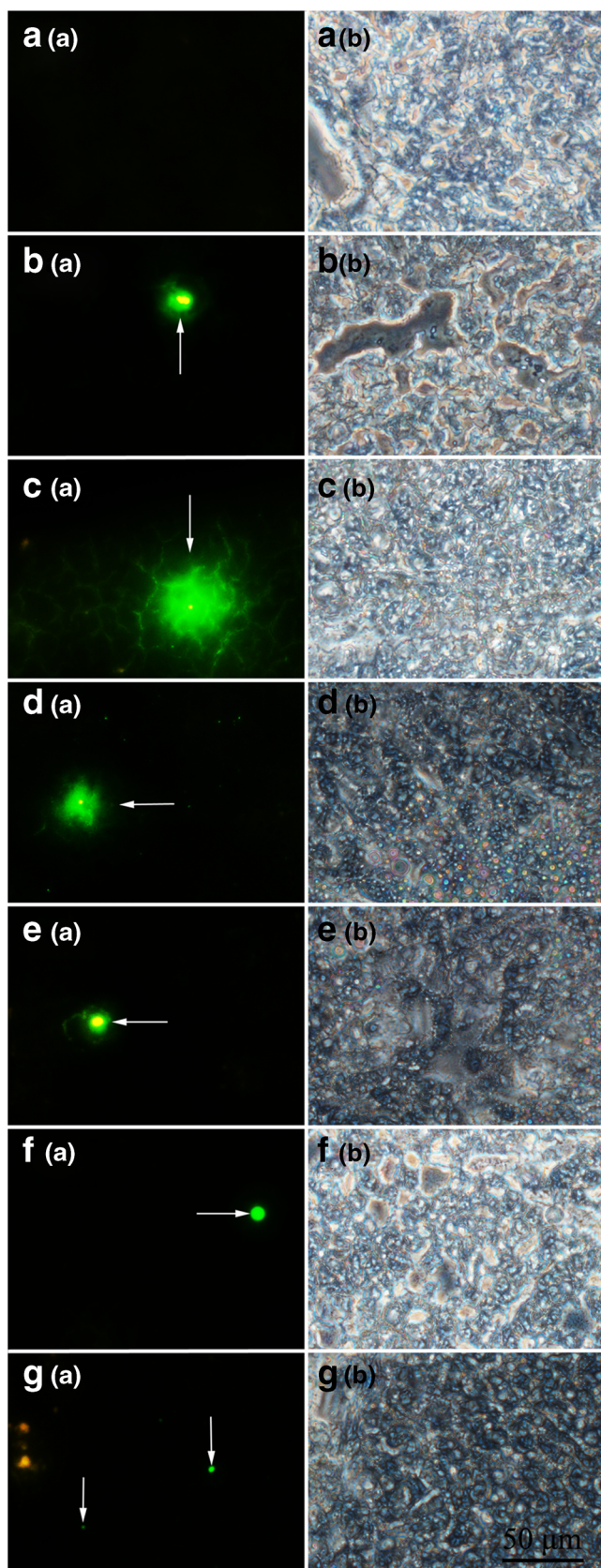


Fig. 5 Fluorescence microscopy images (200 \times) of the mice's liver frozen slices for blank group and experiment groups injected with ECPTNs and HFPTNs simultaneously after 0.5, 1, 2, 4, 8, and 12 h. a images are liver frozen slices of blank group, b–g images are liver frozen slices of experiment group which were picked at 0.5, 1, 2, 4, 8, and 12 h, respectively. The left images are yellow green fluorescence of ECPTNs and HFPTNs with C6 and fluorescein (pointed to by the arrows); the right images are observed from white light channel.

and the cells surrounding the central vein were uniform (Fig. 7a). There was no significant difference between the blank control group and the BPTN group (Fig. 7b and c), which belonged to Grade IV. As shown in Fig. 7d, cancer cells in the FS group were Grade II. Compared with the EMS group (Fig. 7e) and the HSS group (Fig. 7f), a greater number of cancer cells in the EM&HSS group (Fig. 7g) were Grade III. This finding illustrated that the combination therapy was significantly better than single drug administration. Compared with the EPTN group (Fig. 7h) and the HPTN group (Fig. 7i), the majority of cancer cells in the EPTN&HPTN group (Fig. 7j) belonged to Grade I, which further indicated that the combined therapy was superior to that of single drugs. Furthermore, compared with the EM&HSS group, the effect of NPs in combined use was better than that of solutions.

DISCUSSION

Heparin sodium has many biological activities, including anticoagulant activity, angiogenesis and cancer growth inhibition, and the inhibition of the proliferation of vascular smooth muscle cells (27). Clinical study has shown that it is difficult for HS to inhibit cancer growth *via* systemic administration because it cannot reach necessary concentrations in targeted areas. In recent years, research has shown that NPs have good targeting properties, and HS was incorporated into NPs in this study in combination with EPTNs to exert a synergistic effect in the treatment of liver cancer. Because HS is a water soluble drug, it was necessary to select a water soluble fluorescent probe such as eosin and fluorescein, which were more easily encapsulated into NPs with HS to track the *in vitro* cellular uptake and *in vivo* liver targeting capacity of HS. Furthermore, the drug release profiles of NPs marked by fluorescent probes were consistent with those of drug-loaded NPs, which indicated that these NPs would have the same standard behaviour in the *in vitro* cytotoxicity and *in vivo* targeting experiments.

To observe the effects of combined drug treatment on HCC in our study, two drugs were individually incorporated into NPs that was united before injection. The best concentrations and ratios of EMO in combination with HS were first identified through *in vitro* cytotoxicity and cell apoptosis tests, and *in vivo* pharmacodynamics experiments could not achieve better effects. There are a great deal of factors that influence

cells, and the karyoplasm proportion increased significantly. The mice in the normal control group had structural integrity,

Table VI Liver Functional Indexes in the Serum and Liver of the Primary Hepatocarcinogenic mice (n = 8, mean ± SD)

Group	Liver index (g/kg)	Liver function indexes in the serum					Liver function indexes in the liver				
		Y-GT (U/L)	ALT (U/L)	AST (U/L)	ALB (g/L)	T-BIL (μmol/L)	Y-GT (U/gprot)	ALT (U/gprot)	AST (U/gprot)	TP (g/L)	
normal control	42.7 ± 1.9	3.6 ± 1.1	30.4 ± 1.8	98.9 ± 2.0	39.3 ± 2.6	2.4 ± 1.0	0.23 ± 0.14	8.8 ± 1.0	14.5 ± 1.6	15.9 ± 2.3	
blank control	59.6 ± 2.6 ^b	16.5 ± 1.7 ^b	98.4 ± 2.7 ^b	195.6 ± 2.9 ^b	18.9 ± 1.6 ^b	12.1 ± 1.7 ^b	1.97 ± 0.23 ^b	19.9 ± 1.5 ^b	31.9 ± 2.4 ^b	8.5 ± 2.0 ^b	
BPTN	59.4 ± 2.7 ^b	16.6 ± 1.9 ^b	98.7 ± 2.8 ^b	196.3 ± 2.3 ^b	19.2 ± 1.7 ^b	12.3 ± 1.6 ^b	1.96 ± 0.22 ^b	20.1 ± 1.5 ^b	32.2 ± 2.3 ^b	8.6 ± 2.0 ^b	
FS	54.4 ± 2.4 ^a	11.3 ± 1.2 ^a	78.4 ± 2.3 ^a	178.2 ± 2.2 ^a	23.5 ± 1.9 ^a	9.3 ± 1.2 ^a	1.50 ± 0.21 ^a	15.8 ± 1.6 ^a	25.9 ± 2.1 ^a	10.3 ± 2.1 ^a	
EMS	57.3 ± 2.3 ^a	13.5 ± 1.3 ^a	87.6 ± 2.4 ^a	186.5 ± 2.1 ^a	21.4 ± 1.9 ^a	10.2 ± 1.2 ^a	1.66 ± 0.20 ^a	17.4 ± 1.5 ^a	28.6 ± 2.2 ^a	9.5 ± 2.1 ^a	
HSS	58.9 ± 2.5 ^b	15.7 ± 1.9 ^b	95.1 ± 2.7 ^b	193.1 ± 2.4 ^b	20.1 ± 1.7 ^b	11.7 ± 1.6 ^b	1.89 ± 0.24 ^b	19.2 ± 1.5 ^b	31.7 ± 2.4 ^b	8.7 ± 2.0 ^b	
EM&HSS	56.2 ± 2.2 ^a	12.6 ± 1.3 ^a	85.7 ± 2.3 ^a	182.6 ± 2.2 ^a	22.5 ± 1.9 ^a	9.7 ± 1.3 ^a	1.59 ± 0.21 ^a	16.6 ± 1.5 ^a	27.3 ± 2.2 ^a	9.9 ± 2.1 ^a	
EPTN	49.7 ± 2.0	9.2 ± 1.1	66.8 ± 2.2	145.4 ± 2.0	29.3 ± 2.5	6.8 ± 1.0	0.82 ± 0.16	13.3 ± 1.1	20.6 ± 2.0	11.7 ± 2.1	
HPTN	58.6 ± 2.5 ^b	15.2 ± 1.8 ^b	94.3 ± 2.6 ^b	192.3 ± 2.5 ^b	20.8 ± 1.7 ^b	1.87 ± 0.23 ^b	1.89 ± 1.5 ^b	31.4 ± 2.2 ^b	9.1 ± 1.9 ^b	11.7 ± 2.1	
EPTN&HPTN	46.1 ± 2.1	8.3 ± 1.0	59.5 ± 2.0	128.9 ± 1.8	32.3 ± 2.2	5.3 ± 0.8	0.67 ± 0.18	11.7 ± 1.2	17.5 ± 1.8	12.8 ± 2.3	

^a p < 0.05, ^b p < 0.01 versus corresponding EPTN&HPTN group
 Liver index (g/kg) = liver weight of mouse (g)/body weight of mouse (kg)

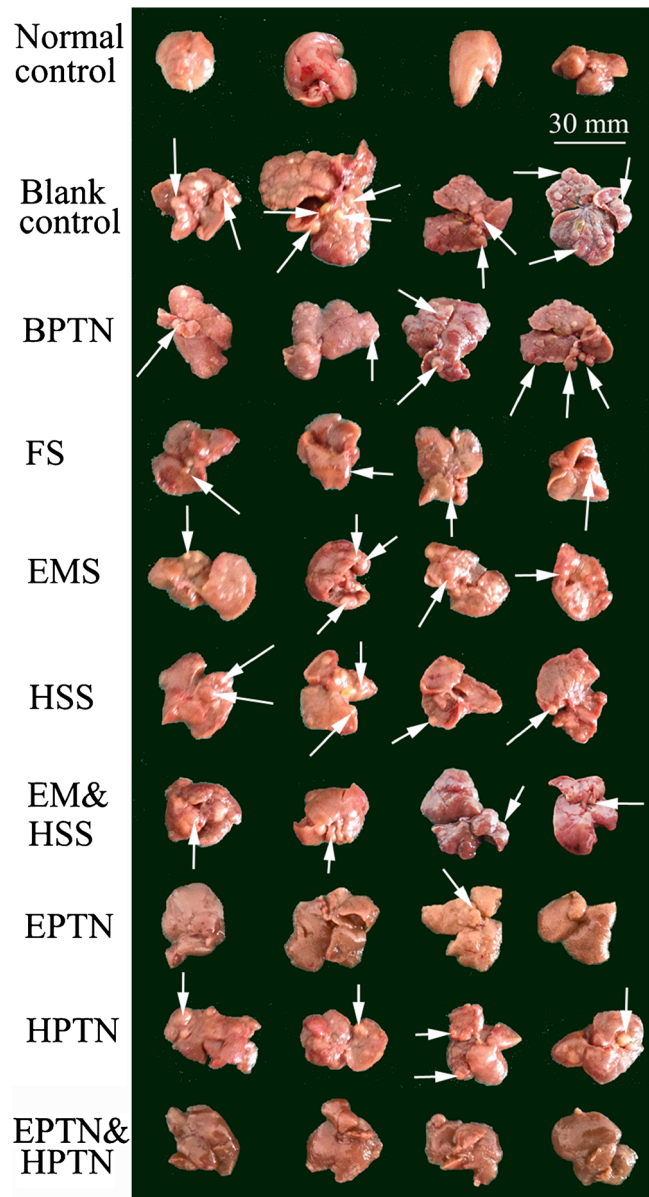


Fig. 6 The morphology images of parts of the livers isolated from the mice in each group after 30 days of administration: the normal control, anticancer efficacy of the blank control (normal saline), BPTN, FS, EMS, HSS, EM&HSS, EPTN, HPTN, EPTN&HPTN on the primary hepatocarcinogenic mice (n = 8). There were some nodules of approximately 12 mm diameter on the livers (pointed to by the arrows).

the preparation process, and NPs were prepared in accordance with the best ratio of two drugs *in vitro*; however, it cannot be guaranteed that the content of the two drugs in the preparation of NPs is the best ratio. The two drugs were individually prepared into NPs to ensure accuracy for *in vivo* pharmacodynamics and to adjust the dosage regimen promptly when the proportion was unsatisfactory.

HS is a water-soluble drug, rendering the NP preparation process complex with the lipid-soluble probe C6 and thus resulting in lower DL and EE. Thus, in this paper, HEPTNs containing eosin as a fluorescent probe were prepared for

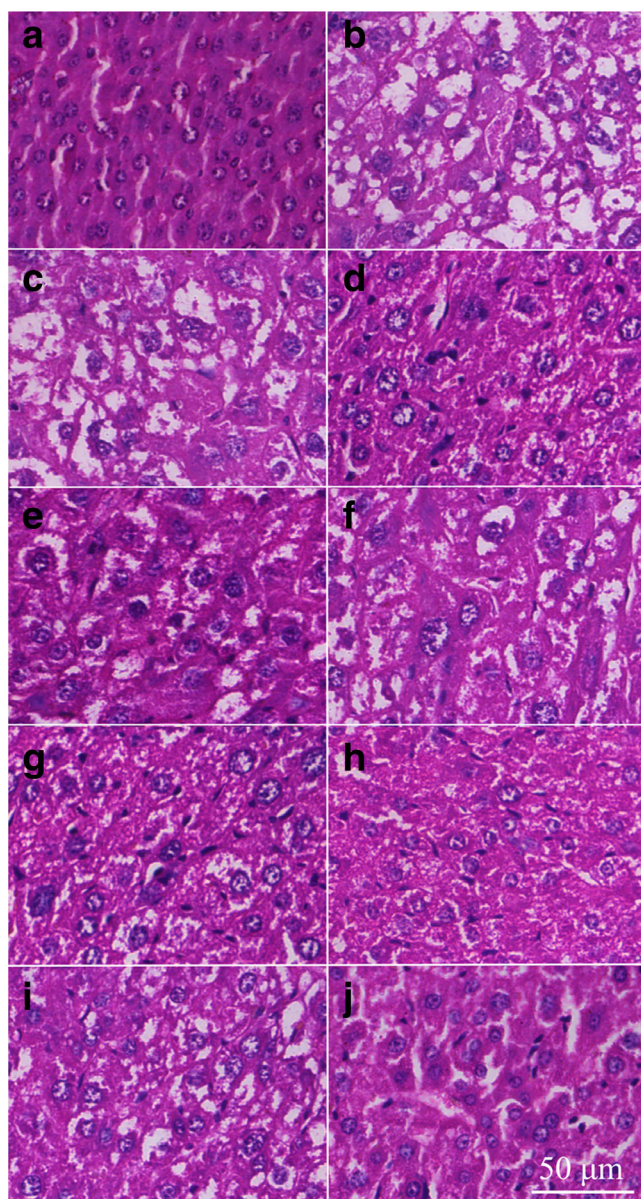


Fig. 7 The ten images were representative of the liver slices of ten groups. **a**: the normal control group; **b**: the blank control group; **c**: the BPTN group; **d**: the FS group; **e**: the EMS group; **f**: the HSS group; **g**: the EM&HSS group; **h**: the EPTN group; **i**: the HPTN group; **j**: the EPTN&HPTN group. The liver slices were H&E stained and observed using microscope (400 \times).

qualitative investigation of cellular uptake by HepG2 cells and HCa-F cells. This was also the first time that two types of NPs were internalized into cells simultaneously. Red fluorescent NPs (red channel) and green fluorescent NPs (green channel) were distributed around the nucleus (blue channel) in two types of cells, which indicated that HS and EMO entered cancer cells *via* cellular uptake. The contents of HS in the two different types of cells were determined quantitatively by RP-HPLC and found to be 60.2 and 47.4%, which is quite similar to the EMO content (61.4 and 48.0%) and demonstrates that HS and EMO were internalized into the cells

simultaneously. Because ECPTNs and HEPTNs were prepared using the same material PLGA-TPGS, leading to similar particle size (150–200 nm) and surface properties, they could be internalized into two types of cells simultaneously and the uptake efficiency was relatively higher at 4 h. In preliminary experiments, most cells died when C6, EMO, eosin, and HS mixed solutions (the same concentrations of ECPTN and HEPTN suspensions) were used for cellular uptake, which illustrated that mixed solutions had strong toxicity. Furthermore, there was almost no fluorescence observed in living cells incubated with the mixed solutions at 4 h. However, the cells grew normally with ECPTNs and HEPTNs, which indicated that NPs can reduce the toxicity of drugs. The free drug and fluorescent probes were in the form of molecules in the mixed solutions, and a few molecules could enter cells because small molecular drugs through cell membrane need active transport carriers and the NPs can be internalized into directly the cancer cells as foreigner. Moreover, the NPs had obvious sustained-release effects (the *in vitro* cumulative release rate of ECPTNs and HEPTNs was 9.8 and 8.7% at 4 h, respectively), and there were approximately 12.2 $\mu\text{g}/\text{mL}$ EMO and 7.7 $\mu\text{g}/\text{mL}$ HS (equivalent to 1.2 IU/mL) in HepG2 cells and approximately 9.5 $\mu\text{g}/\text{mL}$ EMO and 6.1 $\mu\text{g}/\text{mL}$ HS (equivalent to 1.0 IU/mL) in HCa-F cells were released at 4 h, respectively. Therefore, the lower drug concentration and smaller cell toxicity could not affect the observation of cellular uptake. It can be inferred that the two types of NPs could also be absorbed by targeting cells *in vivo*, which laid the foundation for *in vivo* experiments.

HS is a clinically useful anticoagulant, and it also prolongs the survival of cancer patients undergoing antithrombotic therapy (13). The anticancer mechanism of HS may occur through combination with endothelial cells, platelets, and other circulatory systemic cells, or it may interact with cell surface proteins and receptors (such as growth factors, extracellular matrix proteins, chemokines, and enzymes) and be ingested into cells *via* receptor-mediated cellular uptake role to influence gene transcription (28). In our study, we observed that the IR of EPTNs was only 56.27% even if the concentration of EPTNs reached 40 $\mu\text{g}/\text{mL}$. However, the IR of EPTNs increased approximately 5–33% when EPTNs were combined with HPTNs at different concentrations, which indicated that HPTNs had a definite inhibitory effect on HepG2 cells that could improve the inhibitory effect of EPTNs. When EMS was combined with different concentration of HSS, the IR was only increased by approximately 2–12% compared to EMS alone. This minor increase may be because NPs had been taken up directly by cells that did not require active transport. After NPs enter cells, the TPGS in NPs could also inhibit P-gp to improve drug permeability through cell membranes, thus reducing P-gp-mediated MDR in cancer cells, enhancing the absorption of drugs, and increasing the cytotoxicity of drugs to cells (21,22). The present study is the first

report showing *in vitro* that EPTNs combined with HPTNs had better inhibitory effects on HepG2 cells. The best concentration and ratio of EMO combined with HS was selected as reference for *in vivo* experiments.

Apoptosis is also known as programmed cell death (PCD). It is not only essential for normal embryonic organ development and cell proliferation but also plays an important role in various diseases including cancer (29). EMO has anticancer effects, and the effect of combined administration of EMO has been demonstrated (30). In this study, we used Annexin-V/PI fluorescence to detect cell apoptosis. EMO induced the apoptosis of HepG-2 cells, but the effect of HS was not obvious. In Table III, the number of Annexin-FITC stained cells in the EPTN and HPTN group was greater, which indicated more apoptotic cells compared with EMS and HSS. This apoptosis is the likely reason that NPs could be endocytosed directly into HepG2 cells without biological membrane transport and that TPGS could inhibit the MDR of P-gp (21,22). Thus EPTNs and HPTNs could enter the cells, release drugs upon lysosomal activity, and further promote apoptosis. In addition, the proportion of apoptotic cells in the EMO&HSS group was higher than in the EMS and HSS groups, which illustrated that the combination of free drugs had synergistic effects. The results of apoptosis provided the basis for *in vivo* experiments.

In the present study, an RP-HPLC method was established to determine the quantities of HS and EMO in the same biological samples because EMO is a lipid-soluble drug and HS is a water-soluble drug. Because there is no interference between the two drugs, endogenous substances, EMO, and HS can achieve good separation.

In this study, two types of NPs were injected into mice by tail vena injection according to the optimal ratio of ECPTNs and HFPTNs determined *in vitro* assays. The aim was to determine the optimal proportion of the two NPs for targeting the liver at the same time. The concentrations of EMO and HS in the liver were 29.8 $\mu\text{g}/\text{mL}$ and 10.9 IU/mL, respectively, at 1 h, and these levels were the maxima for the study period. The two types of NPs had similar particle size and surface charge and the same carrier material, which could make the two types of NPs target to the liver and release drugs at the same time and thus synergize to inhibit liver cancer.

In this study, EPTNs and HPTNs were prepared by passive targeting agents, and they were controlled *via* the size and surface charge of NPs to achieve passive targeting to the liver. Furthermore, TPGS could improve drug permeability through cell membranes by inhibiting P-gp (21,22), thus enhancing the absorption of drugs and reducing P-gp-mediated MDR in cancer cells. Two types of NPs could not only increase the concentration of drugs in targeting organs and prolong the time of drug action but also reduce the number of drug dosage administrations, and the toxic side effects to non-target organs, thus allowing EMO and HS to have better anticancer activity.

DEN containing nitrite amine groups has dual effects, including toxicity and the induction of cancer. The primary hepatocarcinoma mouse model induced by DEN was simple, and the success rate of induced cancer was higher. The heterotopic transplantation model is one of the most commonly used and most mature hepatocarcinoma models; it is easy to establish and observe, but the growth environment of tumour cells is totally different from that of primary tumours. Furthermore, the heterotopic transplantation model rarely metastasizes. The primary liver cancer model more closely resembles human hepatocellular carcinoma. Although the induction period is very long and the success rate is less than 100%, the location, time, and number of tumours developed are not uniform; and the model is very suitable for studying the etiology and pathogenesis of liver cancer (31). The liver surface of the normal control group was smooth, reddish, and had sharp edges. However, the liver surface of the other groups had different sized white nodules. The diameter of nodules in the EPTN&HPTN group was decreased compared with the other groups. There was no significant difference in the diameter of nodules between the blank control group and the BPTN group, and there were some larger nodules on the surface of the liver.

γ -GT is not expressed in the mature liver cells, and it is often associated with the malignant transformation of cells. In the course of animal liver cancer, γ -GT is regarded as a positive marker of early liver cell variation and the characteristic index of liver precancerous lesions. ALT and AST are mainly distributed in the liver cells, and their levels increase when liver cells are necrotic. The extent of increase is consistent with the degree of liver cell damage, and thus these levels are most commonly used to evaluate liver pathological changes. In addition, T-BIL is mainly used for the differential diagnosis of liver disease and bile duct abnormalities. Furthermore, the decrease of ALB and TP is commonly found in liver cirrhosis with ascites and other liver functional damage. In this study, these liver functional indexes in the experimental groups were significantly different compared to the normal control group, which demonstrated that the hepatocarcinogenic mouse model was established successfully. While the activity of γ -GT, ALT, and AST in the serum and liver were significantly lower and ALB in the serum, TP in the liver were higher for the EPTN&HPTN group compared to the EM&HSS and the blank control groups. This finding indicated that EPTN&HPTN had a better therapeutic effect on liver cancer in mice.

After the injection of FS, the mental state of mice was not good, possibly because FS which is less selective for cancer cells can also kill a large number of normal cells and result in a shorter survival time. However, the EPTN, HPTN, and EPTN&HPTN groups did not have this phenomenon because the NPs improved liver specificity and reduced the toxic side effects to other tissues, and as a result the body weight of

each mouse in the EPTN and EPTN&HPTN groups had a certain extent increased after 30 days of drug administration. At the same time, the liver injury was severe in the experimental group. In a preliminary experiment, the mice were administered once daily; in this case, the drugs were toxic or irritants, and the mortality was higher in the FS, EMS, and EM&HSS groups, which was not conducive to the final result. Therefore, the administration time was reduced to once every 3 days, which reduced the mortality of mice and allowed better investigation of the release of NPs. Compared with the EM&HSS group, the EPTN&HPTN group significantly inhibited the tumour cells. This result was consistent with *in vitro* cytotoxicity and apoptosis assays. NPs allowed sustained release and a high cellular uptake rate. Meanwhile, NPs demonstrate good liver targeting and can increase the drug concentration in the targeting site.

CONCLUSION

In this research, EMO-loaded PLGA-TPGS NPs and HS-loaded PLGA-TPGS NPs, functioning as liver-targeting drug carriers for the delivery of EMO and HS into malignant HCC, were prepared using ultrasonic emulsification-solvent evaporation. In our previous work, EPTNs were prepared and shown to treat liver cancer effectively. However, EPTNs had only been used for cancer therapy and could not suppress vascular proliferation, which is an important factor in the growth, development, and metastasis of tumours. To improve this effect, HPTNs were also prepared and combined with EPTNs to investigate their efficacy as combination therapy. The cancer angiogenesis inhibitor HS could enhance the curative effect of other anticancer drugs reported by many papers. All NPs prepared in this report showed smaller size ranging from 150 to 200 nm, higher DL and EE, and a certain sustained release rate *in vitro*. To assess the *in vitro* internalization by HepG2 cells and HCa-F cells in cellular uptake and *in vivo* liver-targeting experiments, eosin and fluorescein were used as hydrophilic fluorescent probes in NPs for the first time. *In vitro* cytotoxicity and cell apoptosis assays demonstrated that EPTNs combined with HPTNs had better inhibitory effects against HepG2 cells. In addition, the combination of EPTNs and HPTNs showed a strong synergistic effect in animals. Furthermore, we established a primary hepatocarcinogenic mouse model and showed that EPTNs combined with HPTNs had a more pronounced effect on liver cancer *in vivo* compared with EPTN or HPTN administration alone. Therefore, EMO combined with HS showed stronger anticancer effects compared with single drugs, and this was more significant after being incorporated into NPs. This research provides direction for the combination of chemotherapy drugs with traditional Chinese medicine in future clinical cancer treatments.

ACKNOWLEDGMENTS AND DISCLOSURES

This work was supported by the Natural Science Foundation of Liaoning Province, China (No. 2015020308) and the Research Fund for the Doctoral Program of Higher Education of China (No. 20122105120008). The authors are grateful for material support from Dr. Lin Mei at the Academy of Life Sciences, Tsinghua University (Beijing, China). The authors declare no conflicts of interest. The authors alone are responsible for the content and writing of this article.

REFERENCES

1. Forner A, Llovet JM, Bruix J. Hepatocellular carcinoma. *Lancet*. 2012;379(9822):1245–55. doi:10.1016/S0140-6736(11)61347-0.
2. Ferlay J, Shin HR, Bray F, Forman D, Mathers C, Parkin DM. Estimates of worldwide burden of cancer in 2008: GLOBOCAN 2008. *Int J Cancer*. 2010;127(12):2893–917. doi:10.1002/ijc.25516.
3. D'Alessandro LA, Meyer R, Klingmüller U. Hepatocellular carcinoma: a systems biology perspective. *Front Physiol*. 2013;4:28. doi:10.3389/fphys.2013.00028.
4. Jemal A, Bray F, Center MM, Ferlay J, Ward E, Forman D. Global cancer statistics. *CA Cancer J Clin*. 2011;61(2):69–90. doi:10.3322/caac.20107.
5. Tanaka S, Arai S. Molecular targeted therapies in hepatocellular carcinoma. *Semin Oncol*. 2012;39(4):486–92. doi:10.1053/j.seminoncol.2012.05.005.
6. Enguita-Germán M, Fortes P. Targeting the insulin-like growth factor pathway in hepatocellular carcinoma. *World J Hepatol*. 2014;6(10):716–37. doi:10.4254/wjh.v6.i10.716.
7. Feng YM, Feng CW, Chen SC, Hsu CD. Unexpected remission of hepatocellular carcinoma (HCC) with lung metastasis to the combination therapy of thalidomide and cyproheptadine: report of two cases and a preliminary HCC cell line study. *BMJ Case Rep*. 2012;1–5. doi:10.1136/bcr-2012-007180.
8. Joung YK, Jang JY, Choi JH, Han DK, Park KD. Heparin-conjugated pluronic nanogels as multi-drug nanocarriers for combination chemotherapy. *Mol Pharm*. 2013;10(2):685–93. doi:10.1021/mp300480v.
9. Pasqualini JR, Blumberg-Tick J, Nguyen BL. Effect of triptorelin (Decapeptyl) combined with heparin on estradiol levels in MCF-7 mammary cancer cells after incubation with estrone sulfate. *Acta Endocrinol (Copenh)*. 1993;129(3):260–2.
10. Borsig L. Selectins facilitate carcinoma metastasis and heparin can prevent them. *News Physiol Sci*. 2004;19:16–21. doi:10.1152/nips.01450.2003.
11. Cole CL, Rushton G, Jayson GC, Avizienyte E. Ovarian cancer cell heparan sulfate 6-O-sulfotransferases regulate an angiogenic program induced by heparin-binding epidermal growth factor (EGF)-like growth factor/EGF receptor signaling. *J Biol Chem*. 2014;289(15):10488–501. doi:10.1074/jbc.M113.534263.
12. Barash U, Cohen-Kaplan V, Doweck I, Sanderson RD, Ilan N, Vlodavsky I. Proteoglycans in health and disease: new concepts for heparanase function in tumor progression and metastasis. *FEBS J*. 2010;277(19):3890–903. doi:10.1111/j.1742-4658.2010.07799.x.
13. Bereczky B, Gilly R, Rásó E, Vágó A, Timár J, Tóvári J. Selective antimetastatic effect of heparins in preclinical human melanoma models is based on inhibition of migration and microvascular arrest.

- Clin Exp Metastasis. 2005;22(1):69–76. doi:10.1007/s10585-005-3859-6.
14. Su YJ, Tsai MS, Kuo YH, Chiu YF, Cheng CM, Lin ST, *et al.* Role of Rad51 down-regulation and extracellular signal-regulated kinases 1 and 2 inactivation in emodin and mitomycin C-induced synergistic cytotoxicity in human Non-small-cell lung cancer cells. *Mol Pharmacol.* 2010;77(4):633–43. doi:10.1124/mol.109.061887.
 15. Liu HY, Gao M, Xu H, Guan X, Lv L, Deng S, *et al.* A promising emodin-loaded poly (lactic-co-glycolic acid)-d- α -tocopheryl polyethylene glycol 1000 succinate nanoparticles for liver cancer therapy. *Pharm Res.* 2016;33(1):217–36. doi:10.1007/s11095-015-1781-4.
 16. Nagaich S, Khopade AJ, Jain NK. Lipid grafts of egg-box complex: a new supramolecular biovector for 5-fluorouracil delivery. *Pharm Acta Helv.* 1999;73(5):227–36. doi:10.1016/j.biomaterials.2012.06.026.
 17. Win KY, Feng SS. Effects of particle size and surface coating on cellular uptake of polymeric nanoparticles for oral delivery of anticancer drugs. *Biomaterials.* 2005;26:2713–22. doi:10.1016/j.biomaterials.2004.07.050.
 18. Yu L, Bridgers A, Polli J, Vickers A, Long S, Roy A, *et al.* Vitamin E-TPGS increases absorption flux of an HIV protease inhibitor by enhancing solubility and permeability. *Pharm Res.* 1999;16(12):1812. doi:10.1023/A:1018939006780.
 19. Ma Y, Zheng Y, Liu K, Tian G, Tian Y, Xu L, *et al.* Nanoparticles of poly(lactide-co-glycolide)- d- α -tocopheryl polyethylene glycol 1000 succinate random copolymer for cancer treatment. *Nanoscale Res Lett.* 2010;5:1161–9. doi:10.1007/s11671-010-9620-3.
 20. Chen HB, Zheng Y, Tian G, Tian Y, Zeng XW, Liu G, *et al.* Oral delivery of DMAB-modified docetaxel-loaded PLGA-TPGS nanoparticles for cancer chemotherapy. *Nanoscale Res Lett.* 2011;6(1):33–48. doi:10.1007/s11671-010-9741-8.
 21. Guo Y, Luo J, Tan S, Otieno BO, Zhang Z. The applications of Vitamin E TPGS in drug delivery. *Eur J Pharm Sci.* 2013;49(2):175–86. doi:10.1016/j.ejps.2013.02.006.
 22. Mei L, Zhang Z, Zhao L, Huang L, Yang XL, Tang J, *et al.* Pharmaceutical nanotechnology for oral delivery of anticancer drugs. *Adv Drug Deliv Rev.* 2013;65(6):880–90. doi:10.1016/j.addr.2012.11.005.
 23. Jin ZJ. Addition in drug combination. *Acta Pharmacol Sin.* 1980;1(2):70–6.
 24. Sengupta D, Chowdhury KD, Sarkar A, Paul S, Sadhukhan GC. Berberine and S allyl cysteine mediated amelioration of DEN+CC14 induced hepatocarcinoma. *Biochim Biophys Acta.* 1840;2014:219–44. doi:10.1016/j.bbagen.2013.08.020.
 25. Chen Z, Yu D, Liu C, Yang X, Zhang N, Ma C, *et al.* Gadolinium-conjugated PLA-PEG nanoparticles as liver targeted molecular MRI contrast agent. *J Drug Target.* 2011;19(8):657–65. doi:10.3109/1061186X.2010.531727.
 26. Edmondson HA, Steiner PE. Primary carcinoma of the liver: a study of 100 cases among 48 900 necropsies. *Cancer.* 1954;7:462–503. doi:10.1002/1097-0142(1954)057.
 27. Cassinelli G, Lanzi C, Tortoreto M, Cominetti D, Petrangolini G, Favini EZ, *et al.* Antitumor efficacy of the heparanase inhibitor SST0001 alone and in combination with antiangiogenic agents in the treatment of human pediatric sarcoma models. *Biochem Pharmacol.* 2013;85(10):1424–32. doi:10.1016/j.bcp.2013.02.023.
 28. Borsig L. Antimetastatic activities of heparins and modified heparins. *Exp Evid Thromb Res.* 2010;125:S66–71. doi:10.1016/S0049-3848(10)70017-7.
 29. Sgonc R, Gruber J. Apoptosis detection: an overview. *Exp Gerontol.* 1998;33(6):525–33. doi:10.1016/S0531-5565(98)00031-X.
 30. Guo Q, Chen Y, Zhang B, Kang M, Xie Q, Wu Y. Potentiation of the effect of gemcitabine by emodin in pancreatic cancer is associated with survivin inhibition. *Biochem Pharmacol.* 2009;77:1674–83. doi:10.1016/j.bcp.2009.02.021.
 31. Fausto N, Campbell JS. Mouse models of hepatocellular carcinoma. *Semin Liver Dis.* 2010;30(1):87–98. doi:10.1055/s-0030-1247135.